

Mapping Post-Rainfall Recovery in Arid Regions Using a Hierarchical U-Net

Xin Hong

Department of Environmental Sciences and Sustainability, College of Natural and Health Sciences, Zayed University, Abu Dhabi, the United Arab Emirates – xin.hong@zu.ac.ae

Keywords: LULC classification, PlanetScope, urban resilience assessment, urban flooding, deep learning

Abstract

The United Arab Emirates (UAE) experienced an extreme rainfall event between April 15 and 17, 2024, and that resulted in severe flooding in its coastal regions. Dubai was among the most affected regions. This study applies a hierarchical deep learning model on PlanetScope imagery to detect flood inundation, quantify flood extent by land cover, and examine short-term recovery dynamics. While earlier work detailed the methodological development of a hierarchical U-Net model (Hong et al., *in press*), here we emphasize its application for monitoring resilience trajectories in an arid urban environment. Results show that approximately 22 km² of land was flooded, with bare ground and built area most affected, while vegetation demonstrated greater resilience. Recovery dynamics reveal that vegetation and built area recovered rapidly within the first week, whereas bare ground recovered more slowly but continued to improve through the ten-day monitoring period. These findings highlight the importance of integrating fine-resolution satellite monitoring with deep learning approaches to better understand disaster recovery and inform urban resilience planning in desert cities.

1. Introduction

The intense rainfall that swept across the United Arab Emirates (UAE) from April 15 to 17, 2024, resulted in widespread urban flooding and significant disruption in coastal cities, and Dubai was among the most severely impacted regions (Alawlaqi, 2024; Oxford Analytica, 2024; Rannard, 2024; UAEgov [@UAEmediaoffice], 2024). The scale of the event marked the need for a comprehensive assessment of its environmental consequences, particularly in terms of how different land use and land cover (LULC) classes responded to the inundation. This study focuses developing a hierarchical U-Net deep learning architecture for LULC classification in arid, desert environments, and applying this architecture for evaluating the spatial and temporal dynamics of LULC changes in Dubai triggered by this extreme weather event.

This study extends the earlier work of Hong (2025), which used the U-Net backbone model for LULC classification in the aftermath of the April 2024 Dubai floods. While that study showed the feasibility of deep learning for flood impact assessment, it revealed limitations in distinguishing spectrally similar classes, especially vegetation. To address these challenges, the present study proposes a hierarchical U-Net framework—hereafter referred to as *Hierarchical U-Net with Class-Specific Refinement*, which incorporates class-specific expert models and Bayesian smoothing to improve spatial coherence. This approach enhances classification accuracy and boundary delineation. The main objectives of this study are: (1) to develop an enhanced hierarchical U-Net model to classify pre- and post-rainfall LULC patterns using high-resolution satellite imagery, and (2) to monitor the recovery trajectories of various landscape features.

The presented hierarchical U-Net deep learning model was trained on annotated LULC data derived from Sentinel-2 imagery (10 m resolution) and cross-validated against high-resolution PlanetScope imagery (3 m resolution) to ensure alignment with real-world conditions. PlanetScope imagery captured from a pre-rainfall date (April 14) and a series of post-rainfall dates (April 18, 20, 25, 26, and 27) was classified using the trained model. Through this approach, we assessed the extent of flooding and

the degree of recovery across key LULC categories—water, vegetation, built areas, and bare ground. The results offer valuable insights for environmental monitoring and post-disaster planning in rapidly developing arid regions.

2. Methods

2.1 Study Area and Datasets

The study area Dubai City along the southeastern coast of the Persian Gulf was outlined using the boundary shapefile provided by ESRI (2024) and modified to incorporate additional coastal water regions and islands. This area covers around 1,534 km² (Figure 1).

The study utilized PlanetScope imagery (Planet Labs PBC, 2024) to create LULC classification data. This imagery includes eight multispectral bands at a resolution of 3 meters and was captured on a pre-rainfall date of April 14, as well as on post-rainfall dates of April 18, 20, 25, 26, and 27, 2024. The open-access Sentinel-2 LULC classification data from 2023 at a resolution of 10 meters (Karra et al., 2021) was used in the training sample annotation process. Four LULC classes were defined: water, vegetation, built area, and bare ground.

The annotated sample dataset was made from the 2023 Sentinel-2 LULC classification data and manually corrected by cross-referencing the April 14 PlanetScope scene. The resulting sample dataset is composed of four LULC categories: water, vegetation, built-up areas, and bare ground. In total, 1,188 annotated image slices were created, each with dimensions of 256 × 256 pixels and a stride of 128 × 128 pixels, to be used in training the U-Net model.

2.2 Classification Approach

A hierarchical deep learning framework was used to classify PlanetScope imagery into the four LULC classes. The model builds on an earlier U-Net model trained by Hong (2025) and later improved with the incorporation of incorporates class-specific refinement and Bayesian smoothing as detailed in Hong et al. (*in press*). For this paper, only a brief description is

provided: (1) an initial multi-class segmentation identifies all classes; (2) additional expert refinement improves discrimination



Figure 1. The boundary of study area, Dubai city, modified from Hong (2025).

discrimination between spectrally similar categories; and (3) a Bayesian smoothing step enhances boundary coherence. Rather than presenting technical development, this study emphasizes the application of the framework to track post-rainfall changes. The trained model was applied to all PlanetScope scenes, and classification outputs were imported into ArcGIS Pro 3.4 for further analysis.

2.3 Flood and Recovery Analysis

There were three stages in the flood mapping and recovery analysis: (1) detecting flood areas through a pre–post classification comparison, (2) quantifying floods by land cover, and (3) tracking recovery by land cover across a series of post-rainfall dates.

The first stage was flood detection. The pre-rainfall PlanetScope classification (April 14, 2024) was compared with the immediate post-rainfall classification (April 18, 2024) to delineate inundated zones. Using the Change Detection Wizard in ArcGIS Pro 3.4, all pixels that shifted from non-water categories (vegetation, bare ground, or built-up area) to water were flagged as flooded. This procedure provided a spatially explicit flood map at 3 m resolution.

The second stage was flood quantification by land cover. The flooded areas were overlaid with the original LULC classes to determine how different landscapes were affected. Changes were summarized in both absolute area (km^2) and relative share (%) of flooded land within each LULC category. This allowed identification of the most vulnerable land cover types (e.g., bare ground vs. vegetation).

The last stage was tracking recovery by land cover. To assess resilience, the hierarchical U-Net classifications from later dates (April 20, 25, 26, and 27) were compared against the April 18 flood map. Pixels initially classified as flooded were tracked to determine when they reverted back to non-water classes. Cumulative recovery curves were generated for each land cover class to show the proportion of flooded pixels that had recovered by each monitoring date.

3. Results

3.1 Flood Detection

The hierarchical U-Net model demonstrated strong performance across all land cover classes, which produces coherent class boundaries and reducing noise compared to baseline U-Net results in Hong (2025). Figure 2 illustrates this by comparing raw PlanetScope imagery with the corresponding classifications before and after the rainfall event with a focus on a part of the study area. On April 14, bare ground (purple) and built-up areas (orange) were the dominant land cover types, with patches of vegetation (green) and permanent water (blue). On April 18, one day after the storm, extensive new water patches appeared across both bare ground and urban areas, clearly reflecting flood inundation. By April 20, three days later, many urban areas had drained, while low-lying bare ground remained inundated. These panels demonstrate both the visual accuracy of the model and its capacity to capture short-term land cover transitions triggered by flooding.

Building on these classification results, the mapped flood extent was analyzed at the city scale. The flooded areas, where the LULC classes changed from non-water on April 14 to water class on April 18, the day immediately after the rain, were mapped out and displayed in Figure 3. As we can see, most of the flooded areas were concentrated in specific low-lying or non-vegetated zones, such as Ras Al Khor Wildlife Sanctuary along Dubai Creek, coastal zones such as the World Islands, and industrial areas in the southern part of the city. The model also detected small inundate patches within built-up districts, and such localized surface water accumulation may reflect inadequate drainage. These spatial patterns highlight how both natural wetlands and heavily urbanized or industrialized areas became hotspots of flooding.

3.2 Flood Quantification by Land Cover

The second stage of the analysis quantified the extent of flooding by land cover type. The quantitative results of the flooded areas are presented in Figure 4. Overall, approximately 22 km^2 of the land was flooded. Among the flooded land, bare ground accounted for about 14 km^2 (66% of the total), while built-up areas were the second most affected at about 7 km^2 (32%). In contrast, only 0.4 km^2 of vegetation was flooded, and that accounted for 2% of the flooded extent. These results indicate that vegetation demonstrated greater resilience to flooding, whereas bare ground and built-up areas were more vulnerable. The high proportions in bare ground and built area reflect poor infiltration capacity of exposed soils in arid environments and the rapid surface runoff and water pooling in urbanized areas.

3.3 Recovery Tracking by Land Cover

The third stage of the analysis examined how quickly different land cover classes recovered from flooding in the days following the April 2024 rainfall event. Recovery was defined as the percentage of pixels that reverted to their original pre-rainfall class, and was assessed three, eight, and ten days after the storm. While all classes demonstrated a relatively high recovery level within the first three days after the rain, which is 85 percent on average, the pace of recovery varied across land cover types.

The recovery speed by land cover class between successive post-rainfall dates is summarized in Figure 5. Vegetation showed the fastest short-term recovery. Between Day 3 and Day 8, recovery

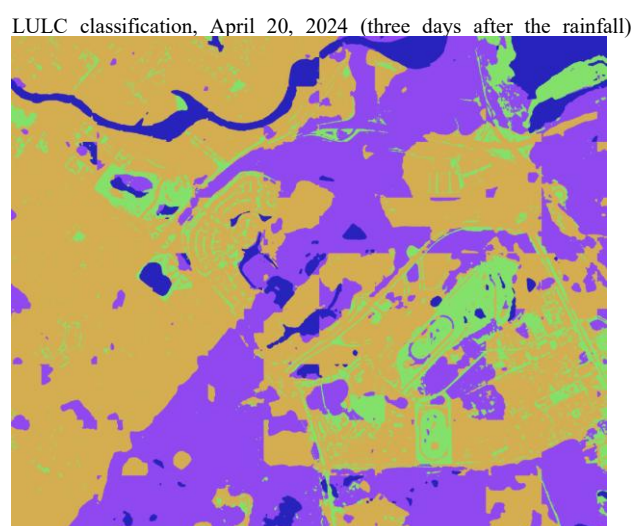
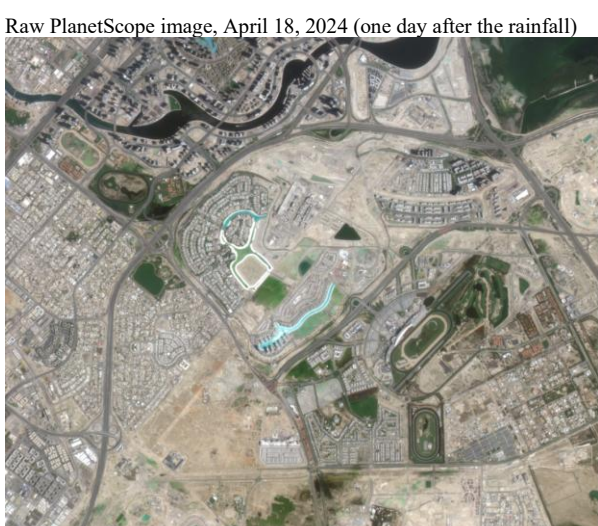
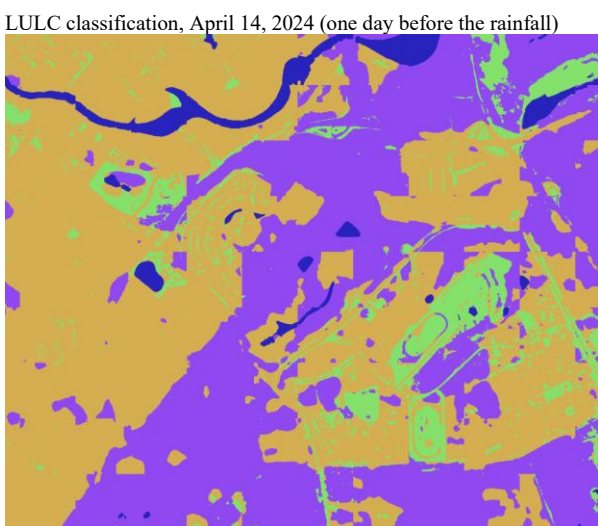
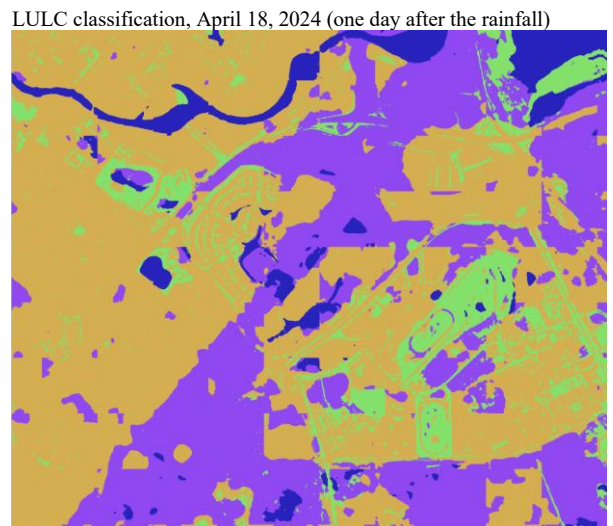
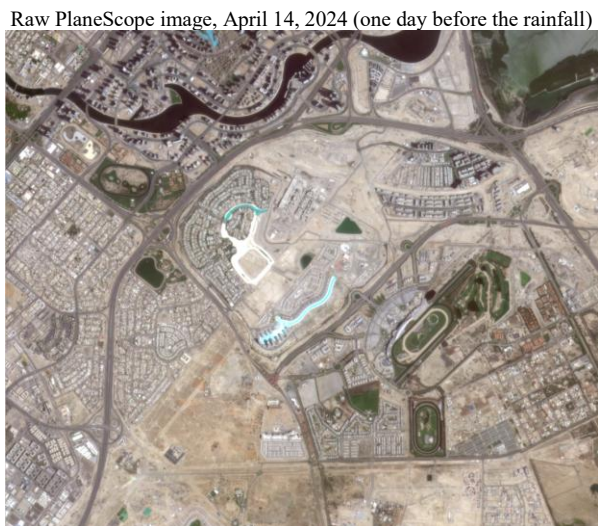


Figure 2. Visual comparison of raw PlanetScope images and hierarchical U-Net classification results before and after the April 2024 rainfall event. The figure highlights transitions from non-water classes (bare ground, built-up, vegetation) to water immediately after the flood and the onset of recovery by April 20.

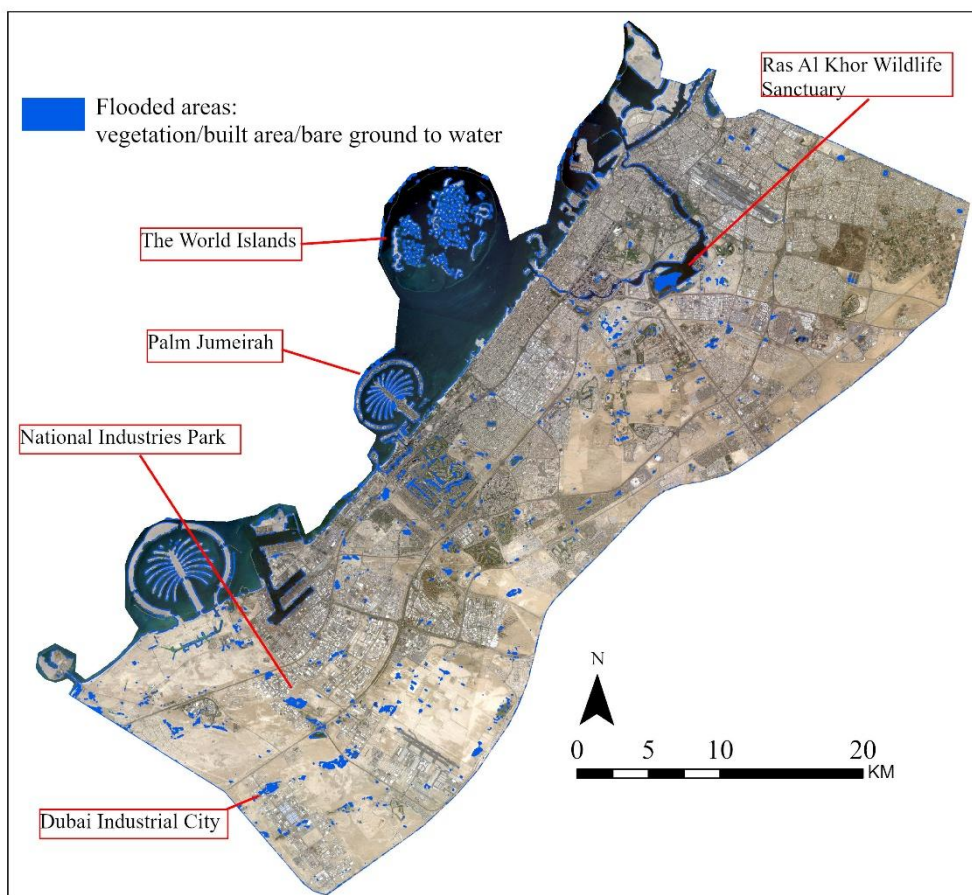


Figure 3. Spatial distribution of flooded areas detected by the hierarchical U-Net model on April 18, 2024. Flooding was concentrated in wetlands, coastal reclamation zones, and industrial estates, with additional localized inundation in urban districts.

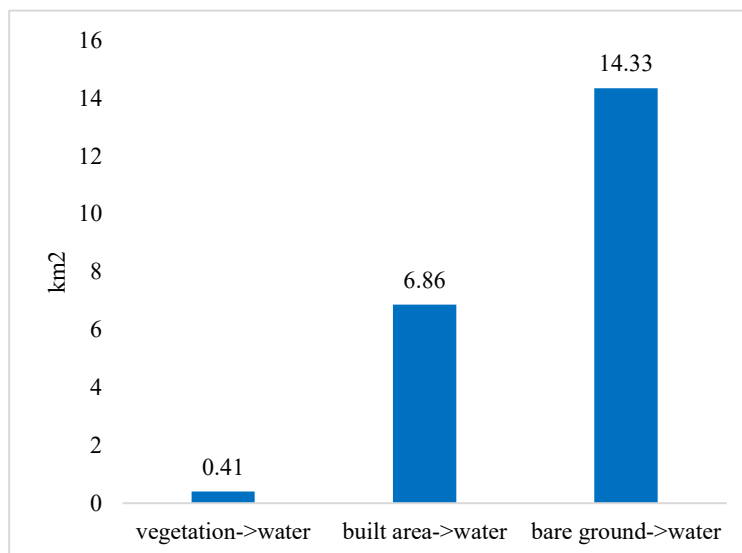


Figure 4. The LULC categorical summary of the flooded areas.

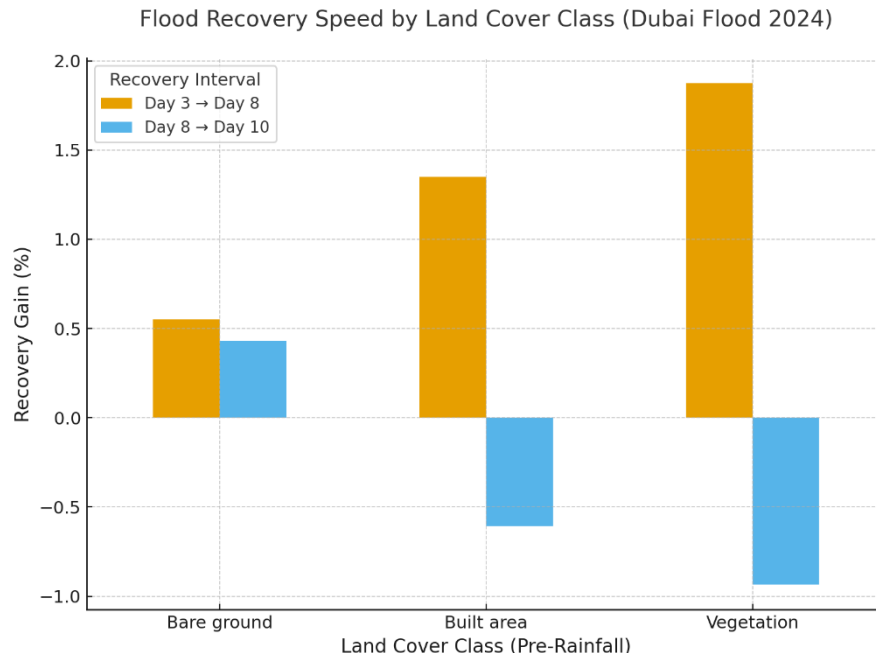


Figure 5. Average recovery speed of different land cover classes between successive post-rainfall dates (Day 3–8 and Day 8–10).

increased by nearly 1.9 percent, which suggests that most vegetated areas drained rapidly immediately after the rain. However, this trend reversed as a slight decline occurred between Day 8 and Day 10. This indicates that while vegetation was initially resilient, some areas likely experienced lingering waterlogging or stress that prevented complete stabilization in the longer term. Built area showed a similar pattern, with recovery improving by about 1.3 percent between Day 3 and Day 8, followed by little to no further improvement in the subsequent two days. This finding reflects the capacity of urban drainage systems to dissipate water quickly, though it also suggests that the majority of recovery processes in urban environments are completed within the first week after flooding.

By contrast, bare ground displayed a slower but more sustained recovery trajectory. Gains were more modest in the first interval, with only about 0.6 percent improvement between Day 3 and Day 8. However, recovery continued to progress after Day 8, with a further 0.4 percent increase by Day 10. This gradual recovery pattern highlights the susceptibility of exposed soils in arid environments to prolonged surface pooling, as well as the longer drainage times required compared to vegetated or urbanized surfaces.

4. Conclusion

This study presented a Hierarchical U-Net with Class-Specific Refinement and Bayesian Smoothing to improve LULC classification and post-flood recovery assessment in arid urban environments. By combining high-resolution PlanetScope imagery and deep learning, we were able to detect inundation zones, quantify flood extent by land cover type, and track short-term recovery dynamics across multiple post-rainfall dates.

Flood detection showed that inundation was mainly in low-lying wetlands, coastal reclamation projects, and industrial areas. The quantification of flood by LULC revealed that bare ground and built area accounted for nearly all the affected land, while vegetation was relatively resilient. In terms of the dynamics of recovery across LULC classes, all land cover types achieved high recovery levels within ten days, but their trajectories differed. Vegetation and built area recovered rapidly within the first week, whereas bare ground recovered more slowly but showed continued improvement through the ten-day period.

The outcomes from this work emphasize that flood vulnerability and resilience are not uniform across the urban landscape. Bare ground was the most susceptible to prolonged flooding probably due to its exposed nature. Built area experienced localized inundation and drained quickly. Vegetation showed high short-term resilience with some longer-term stress effects. By combining fine-scale satellite observations with an enhanced deep learning framework, this study provides an effective approach for mapping floods and monitoring recovery in arid urban environments. Such insights are critical for improving urban resilience planning, guiding flood mitigation strategies, and supporting adaptation to future extreme rainfall events in rapidly developing desert cities.

Acknowledgements

This study was funded by the Zayed University Start-Up Grant. The grant code is 23022.

References

Alawlaqi, A. W. 2024. "We underestimated this storm": UAE residents face electricity, water outages after flooding, heavy rains". Khaleej Times. <https://www.khaleejtimes.com/uae/we>

underestimated-this-storm-uae-residents-face-electricity-water-outages-after-flooding-heavy (3 January 2025)

ESRI. 2024. “United Arab Emirates Region Boundaries”.<https://www.arcgis.com/home/item.html?id=6b25e7dfef5445878fdcd4579c143fd0> (10 May 2024)

Hong, X., Da, L., & Wei, H. (in press). FM-LC: A hierarchical framework for urban flood mapping by land cover identification models. *IEEE Transactions on Geoscience and Remote Sensing*.

Hong, X. 2025. Urban landscape recovery and LULC analysis: A deep learning approach to post-extreme rainfall impacts in Dubai, *Int. Arch. Photogramm. Remote Sens. Spatial Inf. Sci.*, XLVIII-G-2025, 605–610, <https://doi.org/10.5194/isprs-archives-XLVIII-G-2025-605-2025>, 2025.

Karra, K., Kontgis, C., Statman-Weil, Z., Mazzariello, J. C., Mathis, M., Brumby, S. P. 2021. Global land use/land cover with Sentinel 2 and deep learning. 2021 IEEE International Geoscience and Remote Sensing Symposium IGARSS, 4704–4707. <https://doi.org/10.1109/IGARSS47720.2021.9553499>

Oxford Analytica. 2024. Flash floods will increase in frequency in the Gulf. <https://doi.org/10.1108/OXAN-DB286682> (10 May 2024)

Planet Labs PBC. 2024. Planet application program interface: in space for life on earth. <https://api.planet.com>

Rannard, G. 2024. “Deadly Dubai floods made worse by climate change”. BBC News. <https://www.bbc.com/news/science-environment-68897443> (10 May 2024)

UAEGOV [@UAEmediaoffice]. 2024.
<https://t.co/lir6ZS2Dzs> [Tweet]. Twitter.
<https://x.com/UAEmediaoffice/status/1780326720588906951>
(10 May 2024)